Fluorescence and ferroelectric microregions in $KTaO_3$

1989 J. Phys.: Condens. Matter 1 2515

(http://iopscience.iop.org/0953-8984/1/14/007)

J. Phys.: Condens. Matter **1** (1989) 2515–2520. Printed in the UK

Fluorescence and ferroelectric microregions in $KTaO_3$

P Grenier†, G Bernier†, S Jandl†, B Salce‡ and L A Boatner§

† Département de Physique, et Centre de Recherche en Physique du Solide, Université de Sherbrooke, Sherbrooke, Québec J1K 2R1, Canada

‡ Laboratoire de Chimie Physique, Centre d'Etudes Nucléaires de Grenoble, 85 X, 38041 Grenoble Cédex, France

§ Solid State Division, Oak Ridge National Laboratory, Oak Ridge, Tennessee 37830, USA

Received 12 August 1988, in final form 5 December 1988

Abstract. The near-infrared fluorescence of pure and doped $KTaO_3$ samples is studied. In the neighbourhood of 14570 cm^{-1}, 11 peaks are observed at 16 K and are associated with the fluorescence of a Ta^{3+} ion near an O vacancy. In the ferroelectric $KTa_{0.982}Nb_{0.018}O_3$ crystal the fluorescence is not affected below $T_c \simeq 25$ K, indicating that the Ta^{3+} ion in the $KTaO_3$ material is located in a ferroelectric microdomain.

In this paper, we investigate the fluorescence in the near-infrared region of pure $KTaO_3$, $KTa_{0.982}Nb_{0.018}O_3$ and doped $KTaO_3$ samples. This study identifies one of the possible origins of the symmetry-breaking defects responsible for microscopic ferroelectric regions which extend over a few unit cells in pure $KTaO_3$ [1–4].

In [3] it was proposed that residual Nb or Na impurities are at the origin of the ferroelectric regions while the Raman studies in [2, 4] concluded that the Nb impurity is not a major contributor to the disorder-induced scattering resulting from the microdomains.

The optical properties of impurities in ferroelectric and related materials are of great interest since they probe the local crystalline environment [5–11]. A specific infrared emission spectrum was found in Cr-doped and in nominally pure $SrTiO_3$ crystals. It was attributed to the $^2E \rightarrow {}^4A_2$ transition of the Cr^{3+} ion [5, 6, 12]. Below the cubic-to-tetragonal phase transition the ^2E level is split into a doublet by the tetragonal field and the splitting is proportional to $(T_c - T)^{1/2}$ [5]. In [6] an unusually large temperature shift of the zero-phonon line was also observed. It was found that this shift $\Delta E(T)$ and the reciprocal dielectric constant $1/\varepsilon(T)$ have the same temperature dependences.

Infrared fluorescence in Cr-doped $KTaO_3$ has been studied in [7, 8]. These authors also observed a large frequency dependence of the zero-phonon line on temperature with no splitting since $KTaO_3$ retains the cubic centrosymmetric perovskite structure down to liquid-He temperature. Thus the fluorescence of impurities in either $SrTiO_3$ or $KTaO_3$ is very sensitive to the local electric fields and their evolution in the host crystal.

The fluorescence reported in this paper for various pure and doped $KTaO_3$ samples is observed for the first time. The zero-phonon line shows a fine structure of 11 peaks at $T = 16$ K while the vibronic sideband exhibits many structures.

Two pure $KTaO_3$ samples have been used in this work. The first crystal

0953-8984/89/142515 + 06 $02.50

(10 mm × 10 mm × 7 mm) and the second crystal (9 mm × 4 mm × 3 mm) were grown using the top-seeded solution growth and the flux techniques, respectively [13]. We also studied a $KTa_{0.982}Nb_{0.018}O_3$ ferroelectric material (9 mm × 3 mm × 2 mm), obtained by the accelerated crucible rotation technique [14] with $T_c \simeq 25$ K, and five doped $KTaO_3$ samples. Samples were mounted either in a continuous-flow regulated-temperature He cryostat or in a closed-cycle refrigerator. CW Kr and Ar lasers with a pulsed dye laser were used as the exciting source. Emitted light was first analysed with a double monochromator which covers the range 20600–7350 cm^{-1} followed by conventional boxcar and photon counting.

Typical fluorescence spectra of pure $KTaO_3$ and $KTa_{0.982}Nb_{0.018}O_3$ at 16 K are presented in figures 1(*a*) and 1(*b*), respectively. A split zero-phonon line located at around 14567 cm^{-1} is accompanied by vibronic features. We shall first discuss the vibronic spectrum and then the zero-phonon fluorescence line.

Vibrational satellite structures associated with optical transitions of paramagnetic ions in crystals yield information about the phonon frequencies of the host lattice. If the impurity introduces important charge and mass defects, lattice frequencies are modified and many local vibrational modes are present. For $KTaO_3$ the vibronic spectra of Eu^{3+} [15, 16] and of Cr^{3+} [8] have been published with a zero-phonon line at 16920 cm^{-1} and 13414 cm^{-1}, respectively. Much more pronounced and well defined structures were observed as expected in the case of the transition-metal ion Cr^{3+} impurity spectra. Nevertheless, the vibronic frequencies correspond closely for both impurities to the observed phonon frequencies of other studies as given in detail in table 1 of [8].

In our observed fluorescence, vibronic lines are less resolved than those for Cr^{3+}-doped $KTaO_3$. The deduced phonon frequencies are compared with the results of [8] in table 1. Important frequency shifts and many local modes are observed for all the vibronics of pure $KTaO_3$ and $KTa_{0.982}Nb_{0.018}O_3$. This constitutes a clear indication that the impurity at the origin of the vibronics is connected to an important charge and mass defect in our studied samples.

The zero-phonon lines are shown in figures 2(*a*) and 2(*b*), respectively, for $KTaO_3$ and $KTa_{0.982}Nb_{0.018}O_3$ at two typical temperatures, 2.2 and 16 K. Sample quality permits a better resolution of the zero-phonon lines of $KTaO_3$ than of the zero-phonon lines of $KTa_{0.982}Nb_{0.018}O_3$. It is remarkable to note that, even though $KTa_{0.982}Nb_{0.018}O_3$ becomes ferroelectric below 25 K, the energies of the peaks in its fluorescence spectrum at 2.2 K coincide with those of $KTaO_3$.

At $T = 16$ K, 11 peaks are detected between 14550 and 14580 cm^{-1}. The location of the peaks was determined through a Lorentzian lineshape deconvolution. In figure 3, the level scheme, consistent with the observed spectrum at 16 K and its temperature dependence down to 2.2 K, is presented. In [17], different energy diagrams for the d^n ($2 \leqslant n \leqslant 7$) electron configuration of a transition-metal ion in a site of cubic symmetry were calculated within the strong-field approximation. These energy level diagrams give the energy E of the levels as a function of the crystal-field potential Dq scaled by the Racah coefficient B characteristic of the studied ion. The d^2 energy level diagram shown in figure 4 with its fivefold excited-state degeneracy is the only one appropriate to our experimental level scheme in figure 3. It points to a d^2-type transition-metal ion whose fluorescence corresponds to the ^1E, $^1T_2 \rightarrow {}^3T_1$ transition with energy $E = 14567$ cm^{-1}. From the energy level diagram, we calculate $B = 968$ cm^{-1} since $E/B = 15.05$. The degeneracies of the fundamental and excited states are lifted by spin–orbit interaction and low crystal-field symmetry, respectively. The excitation spectrum at 15 K presented in figure 5 locates the $^3T_1 \rightarrow {}^3T_2$ transition at 19050 cm^{-1} and, with $B = 968$ cm^{-1}, Dq is

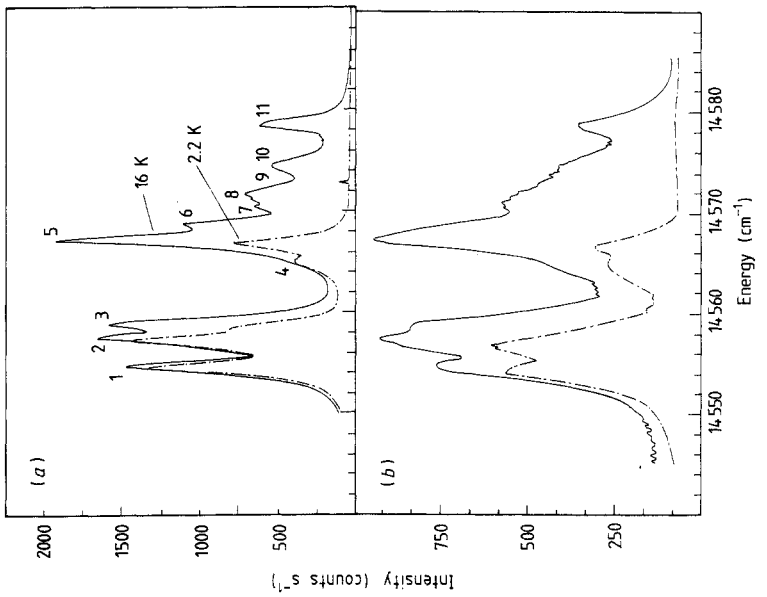

Figure 2. Luminescence of the zero-phonon line of (*a*) $KTaO_3$ and (*b*) $KTa_{0.982}Nb_{0.018}O_3$ at 16 K (——) and 2.2 K (– – –).

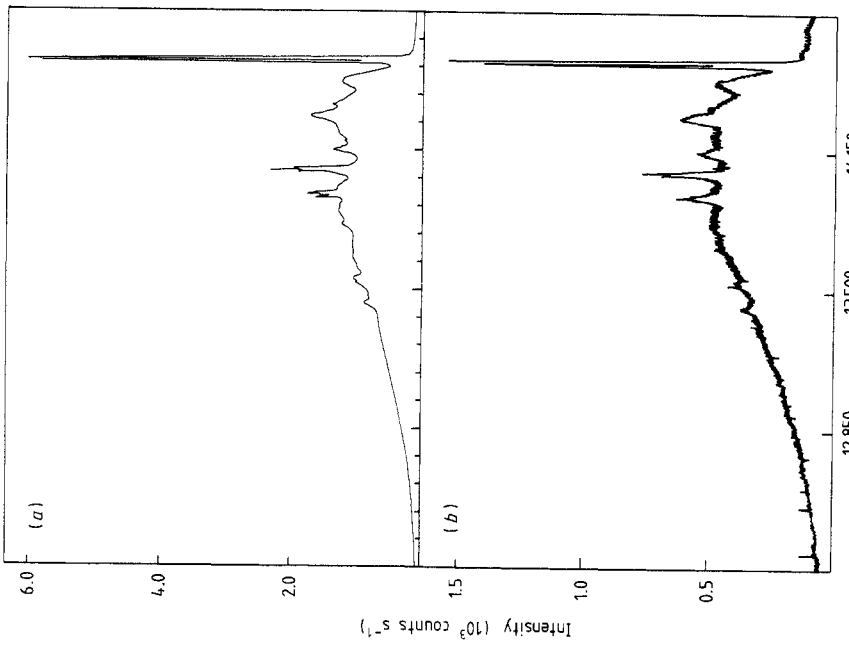

Figure 1. Typical fluorescence spectra of (*a*) $KTaO_3$ and (*b*) $KTa_{0.982}Nb_{0.018}O_3$ at 16 K, both showing the zero-phonon line and the vibronic features.

Table 1. Phonon frequencies appearing in the vibronic spectra of $KTaO_3$ and $KTa_{0.982}Nb_{0.018}O_3$ at 16 K. The uncertainty in the frequency values of this work is ± 4 cm^{-1}.

Phonon frequency, $KTaO_3$ (this work) (cm^{-1})	Phonon frequency, $KTa_{0.982}Nb_{0.018}O_3$ (this work) (cm^{-1})	Phonon frequency, $KTaO_3$ [8] (cm^{-1})
		50
98	96	80
209	203	216
259[a]	257[a]	273
339		330
420[a]	419[a]	447
513[a]	513[a]	543
625[a]	625[a]	645
704	(Weak)	
768	(Weak)	748
873	(Weak)	869
922	(Weak)	
967	(Weak)	975
1024	1021	1017
1135[a]	1132[a]	1099

[a] Local modes.

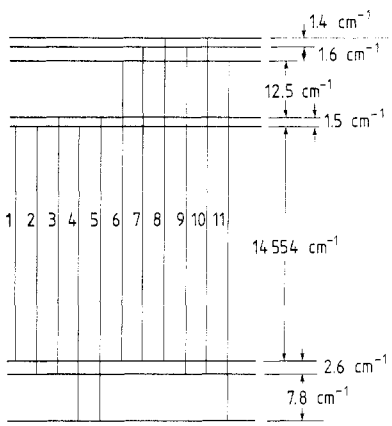

Figure 3. The corresponding level scheme of the impurity zero-phonon line in either $KTaO_3$ or $KTa_{0.982}Nb_{0.018}O_3$.

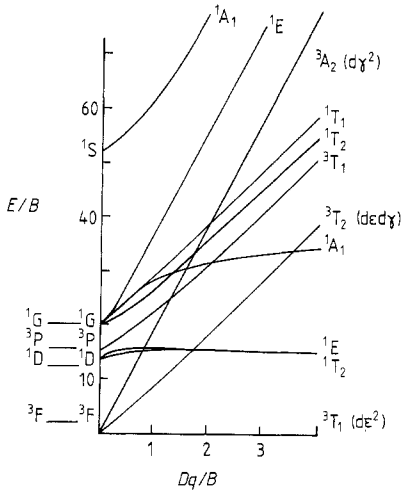

Figure 4. The ion energy levels E/B as a function of the crystal-field strength Dq/B according to the diagram for the d^2 transition-metal ion configuration in [17].

evaluated to be 2140 cm^{-1}. B and Dq have typical values which characterise transition-metal ions of valence 3 in insulators [17].

The measured lifetime of the fluorescence with a pulsed dye laser, between $T = 15$ K and $T = 60$ K, is 3.4 ms. Such a value is indicative of a magnetic dipolar or electric quadrupolar character consistent with the parity of the invoked transition ($^1E_1$, $^1T_2 \rightarrow {}^3T_1$) representations.

The strong similarity of the low-temperature spectra of $KTaO_3$ to those of

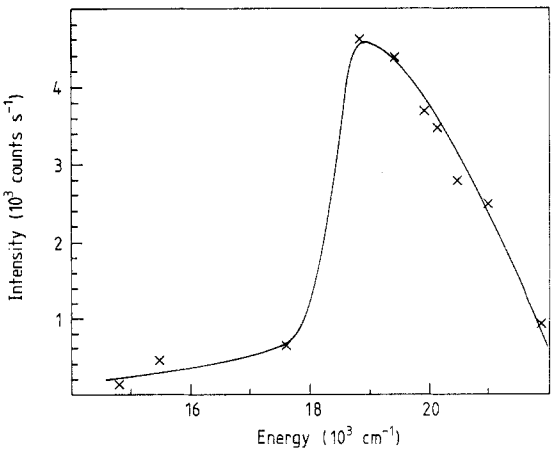

Figure 5. The excitation spectrum of $KTaO_3$ at 15 K. The full curve is given as a visual guide.

$KTa_{0.982}Nb_{0.018}O_3$ at temperatures below its ferroelectric transition ($T_c \simeq 25$ K) indicates that the impurity at the origin of the observed luminescence is insensitive to the ferroelectric transition. This is the case if the impurity pertains to a ferroelectric microdomain in $KTaO_3$. Moreover, the fact that the luminescence is not strengthened but rather weakened in the $KTa_{0.982}Nb_{0.018}O_3$ sample compared with pure $KTaO_3$ excludes the Nb ion as a candidate for the luminescent impurity.

We also studied five doped $KTaO_3$ materials (with Ag (200 ppm), Cu (800 ppm), Co (200 ppm), Na (1000 ppm) and Li (540 ppm)). At around 14570 cm^{-1} the same fluorescence at $T = 16$ K is observed with less resolution than for pure $KTaO_3$ and $KTa_{0.982}Nb_{0.018}O_3$, since the luminescence of doped materials is often quenched by non-radiative processes.

In summary, the luminescent impurity introduces an important charge and mass defect in the lattice and has the properties of a transition-metal ion. It is also located in a ferroelectric microdomain and is universally present in either pure or doped $KTaO_3$ samples, independently of the crystal-growing procedure. We suggest that such an impurity is formed by a complex involving the Ta^{3+} ion (d^2 configuration) located near an O vacancy. Consequently, the O vacancy could be at the origin of the observed microscopic ferroelectric regions cited in the introduction and observed in the thermal conductivity [3] and Raman scattering [2, 4] of $KTaO_3$.

Nb impurities should also produce ferroelectric microdomains in mixed samples $KTa_{1-x}Nb_xO_3$. In fact, long-range order sets in in these materials when the microdomains become sufficiently large. However, these microdomains are not observed in our study since the local probe Ta^{3+} ion is absent following the substitution of the Ta atom by the Nb atom.

A natural extension of this work would be the study of the 14570 cm^{-1} fluorescence, the thermal conductivity and the Raman scattering in pure $KTaO_3$ material where controlled O vacancies are added. The ferroelectric microdomain density should then increase with increasing number of O vacancies.

References

[1] Yacoby Y 1978 *Phys. Rev.* B **31** 275
[2] Prater R L, Chase L L and Boatner L A 1981 *Phys. Rev.* B **23** 221
[3] Salce B, De Goer A M and Boatner L A 1981 *J. Physique Coll.* **42** C6 424

[4] Uwe H, Lyons K B, Carter H L and Fleury P A 1986 *Phys. Rev.* B **33** 6436
[5] Stokowski S E and Schawlow A L 1969 *Phys. Rev.* **178** 457
[6] Stokowski S E and Schawlow A L 1969 *Phys. Rev.* **178** 464
[7] Trepakov V A, Davydov A V, Babinskil A V, Syrnikov P P, Swolenskil G A and Jastrabik L 1986 *Sov. Phys.–Dokl.* **30** 290
[8] Trepakov V A, Babinskil A V, Davydov A V, Syrnikov P P and Jastrabik L 1984 *Sov. Phys.–Solid State* **26** 1885
[9] Houde D, Lépine Y, Pépin C, Jandl S and Brebner J L 1987 *Phys. Rev.* B **35** 4948
[10] Houde D, Jandl S, Grenier P, Pépin C and Lépine Y 1988 *Ferroelectrics* **77** 55
[11] Houde D and Jandl S 1986 *Solid State Commun.* **60** 45
[12] Feng T 1982 *Phys. Rev.* B **25** 627
[13] Belruss V, Kalnajs J, Linz A and Folwieber R C 1971 *Mater. Res. Bull.* **6** 899
[14] Rytz D and Scheel H J 1982 *J. Cryst. Growth* **59** 468
[15] Schaufele R F, Weber M J and Waugh J S 1965 *Phys. Rev.* **140** A872
[16] Yacoby Y and Ling A 1974 *Phys. Rev.* B **9** 2723
[17] Sugano S, Tanabe Y and Kamimura H 1970 *Multiplets of Transition-Metal Ions in Crystals* (New York: Academic)